J Membrane Biol (2007) 220:11–20
DOI 10.1007/s00232-007-9067-3

The Ryanodine Receptor Pore Blocker Neomycin also Inhibits Channel Activity via a Previously Undescribed High-Affinity Ca^{2+} Binding Site

Derek R. Laver · Tomoyo Hamada · James D. Fessenden · Noriaki Ikemoto

Received: 7 November 2006 / Accepted: 21 July 2007 / Published online: 18 September 2007

Abstract In this study, we present evidence for the mechanism of neomycin inhibition of skeletal ryanodine receptors (RyRs). In single-channel recordings, neomycin produced monophasic inhibition of RyR open probability and biphasic inhibition of [^{3}H]ryanodine binding. The half-maximal inhibitory concentration (IC_{50}) for channel blockade by neomycin was dependent on membrane potential and cytoplasmic [Ca^{2+}], suggesting that neomycin acts both as a pore plug and as a competitive antagonist at a cytoplasmic Ca^{2+} binding site that causes allosteric inhibition. This novel Ca^{2+}/neomycin binding site had a neomycin affinity of 100 nM and a Ca^{2+} affinity of 35 nM, which is 30-fold higher than that of the well-described cytoplasmic Ca^{2+} activation site. Therefore, a new high-affinity class of Ca^{2+} binding site(s) on the RyR exists that mediates neomycin inhibition. Neomycin plugging of the channel pore induced brief (1-2 ms) conductance substates at 30% of the fully open conductance, whereas allosteric inhibition caused complete channel closure with durations that depended on the neomycin concentration. We quantitatively account for these results using a dual inhibition model for neomycin that incorporates voltage-dependent pore plugging and Ca^{2+}-dependent allosteric inhibition.

D. R. Laver (✉)
School of Biomedical Sciences, University of Newcastle and Hunter Medical Research Institute, Callaghan, NSW 2308, Australia
e-mail: Derek.Laver@newcastle.edu.au

T. Hamada · J. D. Fessenden · N. Ikemoto
Boston Biomedical Research Institute, Watertown, MA 02472, Australia

N. Ikemoto
Department of Neurology, Harvard Medical School, Boston, MA 02115, Australia

Keywords Ryanodine receptor · Neomycin - Ryanodine binding · Bilayer · Single-channel recording

Introduction

Neomycin is an aminoglycoside antibiotic that blocks Ca^{2+} release from the sarcoplasmic reticulum (SR) of skeletal muscle (Mack, Zimanyi & Pessah, 1992; Yano et al., 1994). Single-channel measurements of cardiac Ca^{2+} release channels (Mead & Williams 2002a, 2002b) show that neomycin can block the pore of these channels when applied to either the cytoplasmic or luminal sides of the membrane. The Ca^{2+} release channels have been dubbed ryanodine receptors (RyRs) (Inui, Saito & Fleischer, 1987; Rousseau, Smith & Meissner, 1987) due to their specific high-affinity binding of ryanodine (RyR1 is the predominant RyR isoform present in skeletal muscle). Ryanodine binding leads to activation of calcium release (Fleischer et al., 1985), which underlies the most potent action of ryanodine on the SR (Jenden & Fairhurst 1969). Ryanodine preferentially binds to RyRs in their open state (Pessah et al., 1986), thus making ryanodine binding a widely used assay for RyR activity. The ryanodine binding site has been located in the 76-kDa region of RyR1 between amino acid position 4475 and the C terminus, a region which contains the putative channel pore (Wang et al., 1996).

Neomycin also binds to this C-terminal 76-kDa region of RyR1 (Chen et al., 2002). Neomycin is believed to block the channel via electrostatic interactions between the negatively charged groups within the pore and the positively charged amino groups on neomycin (Xu et al., 2006). Thus, neomycin may serve as an elecrostatic "plug" of the Ca^{2+} conductance pathway of the channel pore, as has been suggested for the cardiac isoform (RyR2) (Mead &

Williams 2004). However, RyR inhibition by neomycin may not necessarily be targeted to the Ca^{2+} pore alone. As described in our earlier report (Yano et al., 1994), neomycin blockade of depolarization-induced Ca^{2+} release from isolated triads takes place at much lower neomycin concentrations compared to inhibition of polylysine-induced Ca^{2+} release. This suggests that neomycin might bind to another site(s) in addition to the channel portion of the receptor. Moreover, the effects of neomycin on RyR activity as determined by different assays are quite different. Neomycin is reported to produce complete inhibition of Ca^{2+} release from SR vesicles with both monophasic and diphasic concentration dependence (Calviello & Chiesi 1989; Mack et al., 1992), whereas neomycin only produces patial inhibition of ryanodine binding with a biphasic concentration dependence (Mack et al., 1992). This finding also has been taken to indicate multiple modes for neomycin inhibition, although the precise nature of these mechanisms is unknown.

In order to elucidate the mechanisms of neomycin inhibition, we investigated the effect of neomycin on channel activity by measuring single-channel currents in lipid bilayers and [^{3}H]ryanodine binding to SR vesicles at various Ca^{2+} concentrations.

Experimental Procedures

Preparation of SR Vesicles

For [^{3}H]ryanodine binding assays and single-channel measurements, SR vesicles were prepared from New Zealand rabbit back paraspinous and hindleg skeletal muscle (Pel-Freez Biologicals, Rogers, AR) using the method of differential centrifugation as described previously (Ikemoto, Kim & Antoniu, 1988). Microsomes from the final centrifugation were homogenized in 0.3 M sucrose, 0.15 M KCl, proteolytic enzyme inhibitors (0.1 mM phenylmethylsulfonyl fluoride, 1 μg/ml leupeptin, 2 μg/ml soybean trypsin inhibitor) and 20 mM morpholinoethanesulfonic acid (pH 6.8) to a final concentration of 15-30 mg/ml; snap-frozen in liquid N_2; and stored at –80°C.

For some single-channel measurements, SR vesicles were prepared from back paraspinous and hindleg skeletal muscle of New Zealand rabbit skeletal muscle using techniques based on those of Chu et al. (1988), as previously described by Kourie et al. (1996). Briefly, cubes of muscle were homogenized in a Waring (New Hartford, CT) blender in homogenizing buffer (20 mM imidazole, 300 mM sucrose, pH 7.1, with HCl) and centrifuged (11,000 x 3 *g*, 15 min), and the pellet was resuspended, rehomogenized and centrifuged as above. The supernatant was filtered through cotton gauze and pelleted by centrifugation (110,000 x 3 *g* for 60 min) to yield a crude microsomal fraction, which was fractionated by loading onto a discontinuous sucrose gradient. Heavy SR vesicles were collected from the 35–45% (w/v) interface, snap-frozen and stored at -80°C. The conductance data obtained from both SR vesicle isolation methods were indistinguishable from each other.

[^{3}H]Ryanodine Binding Assay

Rabbit skeletal muscle SR vesicles (0.5 mg/ml in a final volume of 0.1 ml) were incubated in a solution containing 10 nM [^{3}H]ryanodine (50-100 Ci/mmol; Perkin-Elmer Life Sciences, Oak Brook, IL) at various concentrations of free Ca^{2+} in 0.23 M $CsCH_3O_3S$, 20 mM CsCl, 1 mM AMP-PCP and 5 mM *N*-tris [hydroxymethyl]methyl-2-aminoethanesulfonic acid (TES, pH 7.2; MP Biomedicals, Solon, OH) at 22°C for 12 h. The free [Ca^{2+}] was buffered with 1 mM 1,2-bis(*o*-aminophenoxy)ethane-*N,N,N′,N′*-tetraacetic acid tetra potassium salt (BAPTA; Molecular Probes, Eugene, OR) and titrated with $CaCl_2$ (added $CaCl_2$ plus contaminating calcium estimated to be 10 μM). When neomycin was used, the SR was preincubated with neomycin 5 min before starting the assay reaction. Samples were filtered onto glass fiber filters (Whatman GF/B, Clifton, NJ) and washed three times with 2.5 ml (in each washing step) of distilled water. The filters were then placed in scintillation vials containing 4 ml of Ecoscint A scintillation mixture and counted in a Beckman (Fullerton, CA) LS 3801 counter. Specific binding was calculated as the difference between the binding in the absence (total binding) and the presence (nonspecific binding) of 20 μM nonradioactive ryanodine. All other reagents and chemicals were obtained from Fisher (Orangeburg, NY), Invitrogen (Carlsbad, CA) and Sigma (St. Louis, MO). The assays were carried out in duplicate, and each data point was obtained by averaging the duplicates three to ten experiments.

Single-Channel Measurements

Lipid bilayers were formed from phosphatidylethanolamine and phosphatidylcholine (8:2 wt/wt; Avanti Polar Lipids, Alabaster, AL) in *n*-decane (50 mg/ml; ICN Biomedicals, Costa Mesa, CA) across an aperture of 150–250 μm diameter in a Delrin cup. During SR vesicle incorporation, the *cis* (cytoplasmic) solution contained 250 mM Cs^+ (230 mM $CsCH_3O_3S$, 20 mM CsCl), 1.0 mM $CaCl_2$ and 500 mM mannitol, while the *trans* (luminal) solution contained 50 mM Cs^+ (30 mM $CsCH_3O_3S$, 20 mM $CsCl_2$) and 1 mM $CaCl_2$. The osmotic gradient across the membrane and the Ca^{2+} in the *cis* solution aided vesicle fusion with the

bilayer. After detection of RyRs in the bilayer, the [$CsCH_3O_3S$] in the *trans* solution was increased to 230 mM (i.e., establishing 250 mM Cs^+ in both *cis* and *trans* baths) by means of aliquot addition of 4 M stock solution. When [Ca^{2+}] was ≤100 μM (this was the case for most experiments), the composition of the *cis* solution was altered by continuous local perfusion of Ca^{2+}-buffered, mannitol-free solutions via a tube placed in close proximity to the bilayer (O'Neill, Sakowska & Laver, 2003). Otherwise, composition was changed by means of aliquot additions of stock solutions. Cesium salts were obtained from Aldrich Chemical Company (Milwaukee, WI), mannitol was obtained from Ajax Chemicals and $CaCl_2$ was from BDH Chemicals (Toronto, Canada). Unless otherwise stated, solutions were pH-buffered with 10 mM TES (MP Biomedicals) and solutions were titrated to pH 7.4 using CsOH (optical grade, MP Biomedicals). Free [Ca^{2+}] ≤3 μM was buffered with 4.5 mM BAPTA and titrated with $CaCl_2$. A Ca^{2+} electrode (Radiometer, Copenhagen, Denmark) was used to measure free [Ca^{2+}] >0.1 μM and determine the apparent association constants for BAPTA and Ca^{2+}. At lower concentrations, free [Ca^{2+}] was calculated using the apparent association constants for BAPTA and Ca^{2+}. The concentrations of $CaCl_2$ and BAPTA stock solutions were calibrated to better than 1% accuracy by titration against a Ca^{2+} standard (Fluka, Buchs, Switzerland).

Bilayer potential was controlled using an Axopatch 200B amplifier (Axon Instruments, Burlingame, CA). Electrical potentials are expressed using the standard physiological convention (i.e., cytoplasmic side relative to luminal side at virtual ground). Single- and multichannel recordings were obtained using bilayer potential differences of ±40 m*V*. For measurements of unitary current and open probability, the current signal was digitized at 5 kHz and low pass-filtered at 1 kHz with a gaussian digital filter. Open probability (p_o) was measured by the 50% threshold detection method. Analysis was carried out using Channel2 software (P. W. Gage and M. Smith, Australian National University, Canberra, Australia). Unless otherwise stated, data are presented as mean ± standard error of the mean (SEM).

Hidden Markov Model Analysis of Single-Channel Recordings

Detailed analysis of channel open, substate and closed durations was made using the hidden Markov model (HMM) algorithm (Chung et al., 1990). HMM finds the maximum likelihood estimate of the channel current transitions present in the record and provides for the determination of channel substate amplitudes, probabilities and transition rates. The algorithm is based on the assumption that the channel current signal is the sum of a first-order finite state Markov process and white, uncorrelated, gaussian noise of known variance. Analysis was carried out on single-channel recordings, with steady baseline, varying in duration by 5-10 s.

Results

Neomycin Inhibits RyR1 via Two Distinct Mechanisms

We determined the effect of increasing cytoplasmic (i.e., *cis*) neomycin concentrations on RyR1 Ca^{2+} channels in the presence of *cis* 2 mM ATP at various [Ca^{2+}] (1 nM-1 mM) and at two different holding potentials (40 and –40 m*V*, Figs. 1 and 2). Neomycin inhibited RyR1 channel p_o without decreasing the maximum conductance level. Inhibition was completely reversed when neomycin was washed out (*not shown*). The concentration of neomycin required for half-maximal inhibition of p_o (IC_{50}) increased with increasing *cis* [Ca^{2+}] (Fig. 2). The IC_{50} value for neomycin inhibition was plotted as a function of the Ca^{2+} concentration at the two holding potentials tested (Fig. 3). Neomycin blockade of the Ca^{2+} channel was clearly influenced by two parameters: (1) the holding potential across the lipid bilayer and (2) the Ca^{2+} concentration on the cytoplasmic (*cis*) side of RyR1. At [Ca^{2+}] below 1 μM, the IC_{50} increased with increasing Ca^{2+} concentration, as one would expect for a mechanism involving competition between Ca^{2+} and neomycin, which has little or no voltage dependence. However, the [Ca^{2+}] dependence of the IC_{50} plateaued at higher [Ca^{2+}], and the level of this plateau had a strong voltage dependence. This feature of the data is indicative of a mechanism in which neomycin does not compete with Ca^{2+} but, instead, involves electrostatic plugging of the Ca^{2+} channel by neomycin, as proposed by Mead & Williams (2004) (*see* Discussion). Therefore, we propose two mechanisms for RyR1 inhibition by neomycin: (1) electrostatic *plugging* of the Ca^{2+} channel pore characterized by its voltage dependence and (2) a novel *allosteric inhibition* due to competition of neomycin with Ca^{2+} to a site on RyR1 represented by the Ca^{2+}-dependent portion of the curve.

In order to quantitatively account for our results, we postulate kinetic schemes for the two mechanisms (schemes I and II in Fig. 4). The allosteric inhibition in which neomycin (N) binds to a cytoplasmic Ca^{2+} site (*C* site) is given in scheme I. The voltage-dependent plugging of the pore (at the *P* site) by the neomycin molecule is given by scheme II. The combination of these two mechanisms is represented by scheme III, where neomycin binding to either the *P* or *C* site inhibits single-channel activity. This model was able to accurately fit the data in

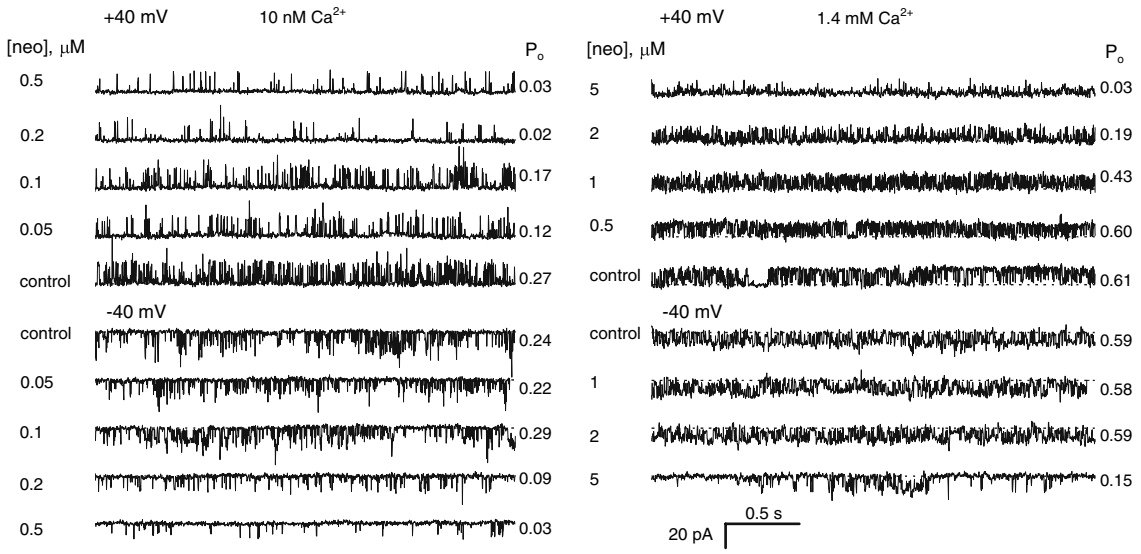

Fig. 1 Bilayer recordings showing neomycin inhibition of RyR1 in the presence of cytoplasmic additions of 2 mM ATP with either 10 nM (three channels) or 1.4 mM (a single channel) Ca^{2+} and either +40 (*upper traces*) or –40 (*lower traces*) m*V* holding potentials. The neomycin concentrations are given in micromolar at the left of each trace, and the open probability values are given at the right of each trace. Channel openings are indicated as upward deflections at 40 m*V* holding potential and downward deflections at –40 m*V*

Figure 3 with only three adjustable parameters: the neomycin and Ca^{2+} affinities at the *C* site and the neomycin affinity of the *P* site. The equations for neomycin inhibition and the parameter values are given in Table 1. The model predicts that at $[Ca^{2+}] < 1$ μM the neomycin binding affinity of the *C* site is the main determinant of the neomycin IC_{50}. At higher $[Ca^{2+}]$, Ca^{2+} competition lowers the apparent affinity of neomycin binding to the *C* site enough to unmask the voltage-dependent, Ca^{2+}-independent pore plugging mechanism, which then sets the upper limit to IC_{50} seen in the micromolar $[Ca^{2+}]$ range.

HMM analysis (*see* Experimental Procedures) of single-channel recordings revealed that the two neomycin inhibition mechanisms are associated with quite distinct forms of channel closures, each characterized by different gating kinetics. Figure 5a shows an example of allosteric inhibition of RyR1 caused by neomycin in the presence of 10 nM cytoplasmic Ca^{2+} and 2 mM ATP at +40 m*V*. Amplitude histograms compiled from extended recordings (>10 s) exhibit two major peaks corresponding to the open and closed states of the RyR. Addition of neomycin caused a reduction in the open state probability, which was countered entirely by an increase in the closed state probability. We were unable to resolve a difference between the conductances of the neomycin inhibited state and the native closed state of the channel. Channel opening and closing rates were derived from HMM analysis of single-channel recordings, and these are shown in Figure 5b and c. Neomycin inhibition was due primarily to a decrease in the channel opening rate (Fig. 5c) and, to a lesser extent, an increase in the channel closing rate (Fig. 5b).

Figure 6a shows the effects of neomycin inhibition of RyR1 in the presence of 100 μM cytoplasmic Ca^{2+} and 2 mM ATP at +40 m*V*, where it was expected that neomycin plugging of the channel pore is the main inhibition mechanism. Under these conditions, RyR1 is strongly activated in the absence of neomycin. Amplitude histograms and HMM substate analysis indicate that RyRs typically undergo transitions from the fully open state to closed state and to a lesser extent undergo transitions to subconductance states (S1 = 33 ± 2% and S2 = 70 ± 2% of the fully open conductance with probabilities of 0.13 ± 0.03 and 0.12 ± 0.02, respectively; mean of five experiments). Addition of neomycin decreases the open state probability of RyR1, which was countered primarily by an increase in the probability of the S1 substate. The probability of the S2 substate was independent of the neomycin concentration. Neomycin increased S1 substate probability via an increase in the transition rate from the open state (O) to the S1 substate (Fig. 6b), whereas neomycin had a relatively small effect on the S1 to O transition rate (Fig. 6c). Neomycin-induced substate activity was observed at $[Ca^{2+}] \geq 0.1$ μM at +40 m*V* but was not detected below 100 μM Ca^{2+} at –40 m*V*. Thus, it appears that neomycin plugging of the channel pore induces brief (1-2 ms) conductance substates (S1 state in scheme II), whereas allosteric inhibition causes complete channel closure with durations that depended on the neomycin concentration (C state in scheme I).

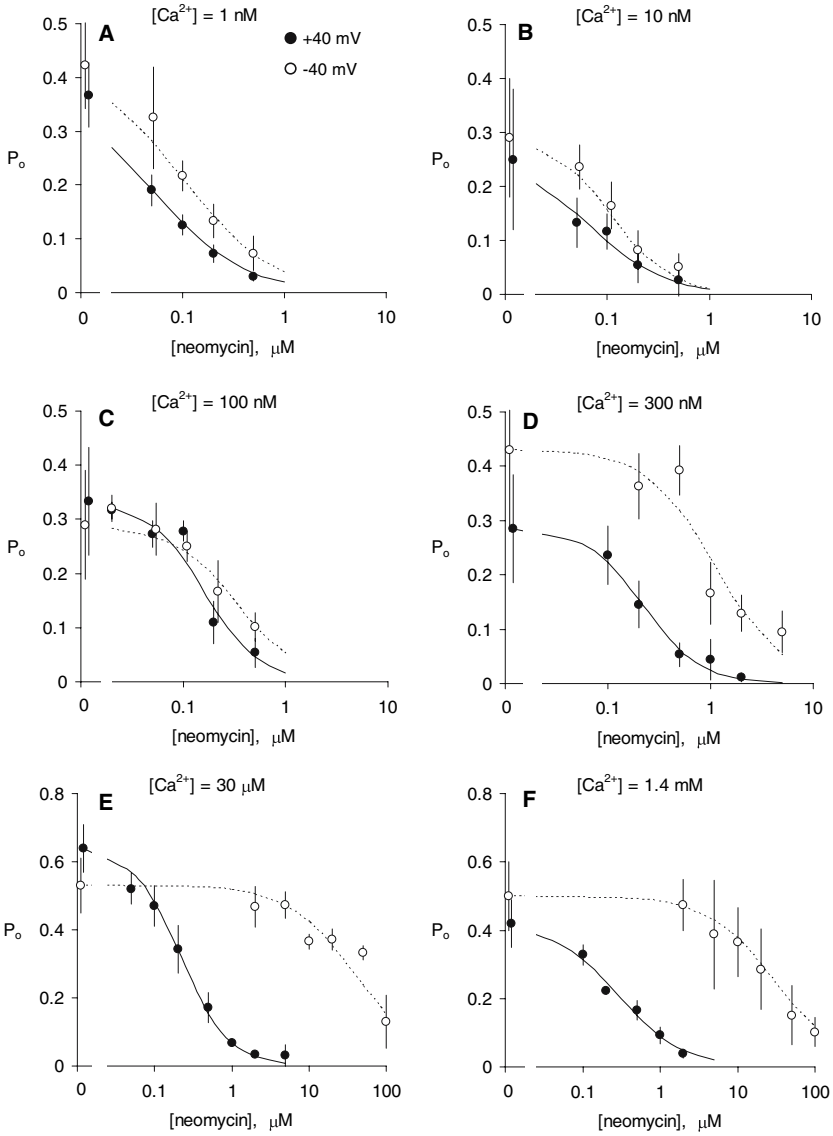

Fig. 2 Effects of increasing concentrations of neomycin on the open probability, p_o, of RyR1 Ca^{2+} channels at two different holding potentials across the lipid bilayers over a range of cytoplasmic [Ca^{2+}] (**a-f**). Each data point was obtained by averaging three to nine experiments. Curves (*solid*, +40 m*V*; *dashed*, –40 m*V*) show Hill fits to the data using the equation $P_o = P_{\max}/(1 + ([neomycin]/IC_{50})^n)$ where P_{max} is the p_o under control conditions, IC_{50} is the half-inhibitory neomycin concentration and n is the Hill coefficient, which ranged 1–1.5

Is Allosteric Inhibition Mediated by the Previously Described Ca^{2+} Activation Site?

To investigate the possibility that neomycin binds at the classical Ca^{2+} activation site (1 μM affinity), we compared the Ca^{2+} dependence of the IC_{50} values for inhibition by neomycin (at –40 m*V*) and Mg^{2+} under equivalent conditions (Fig. 7). (It has been previously shown that Mg^{2+} inhibits RyR1 by competing with Ca^{2+} for the activation site [Laver, Baynes & Dulhunty, 1997].) The data were normalized to their respective IC_{50} values at 1 nM Ca^{2+}. If neomycin and Mg^{2+} bind to different Ca^{2+} sites, then the two data sets in Figure 7 will be different according to the following reasoning. The apparent affinity of neomycin (K'_N, dissociation constant) at a Ca^{2+} site is $K'_N = K_N(1 + [Ca^{2+}]/K_{Ca})$. If normalized for K'_N at low [Ca^{2+}] as done in Figure 7, we get $K'_N/K_N = (1 + [Ca^{2+}]/K_{ca})$. Thus, the differences in the Ca^{2+} dependence of the relative IC_{50} for neomycin (K'_N/K_N) becomes a sole function of K_{Ca}, i.e., the affinity for Ca^{2+} of that site. Applying the same reasoning to the Mg^{2+} site, the relative IC_{50} for Mg^{2+} is $K'_{Mg}/K_{Mg} = (1 + [Ca^{2+}]/K_{ca})$. Therefore, if K_{Ca} obtained from neomycin and Mg^{2+} experiments are different, then neomycin must bind to a site with a different Ca^{2+} affininity from the site to which Mg^{2+} binds. Hence, neomycin and Mg^{2+} bind to different Ca^{2+} sites. Figure 7 shows that this is indeed the case. The Ca^{2+}-dependent increase in the IC_{50} for neomycin is much larger than that for Mg^{2+}. The Ca^{2+} binding affinities to the neomycin and Mg^{2+} sites were determined by fitting the above theory to the IC_{50} (neomycin) *vs.* [Ca^{2+}] data in Figure 7. The Ca^{2+} affinities for the neomycin and Mg^{2+}

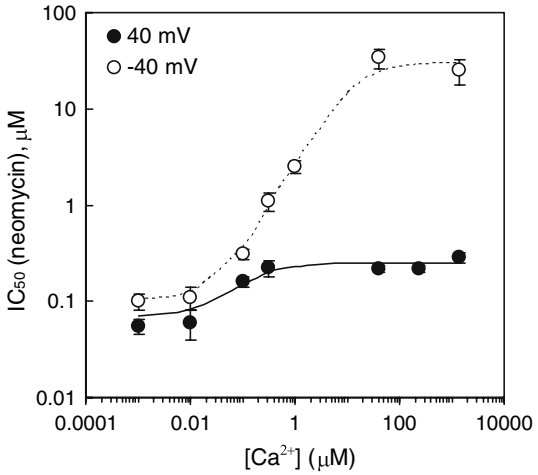

Fig. 3 The $[Ca^{2+}]$ dependence of IC_{50} for neomycin inhibition of RyR1 in the presence of 2 mM ATP at two membrane potentials across the lipid bilayer. *Dashed* and *solid curves* show predictions of scheme III (*see* Fig. 4) using the parameters shown in Table 1 (*solid curve*, +40 m*V*; *dashed curve*, –40 m*V*). Each IC_{50} value was obtained from Hill fits from the data shown in Figure 2

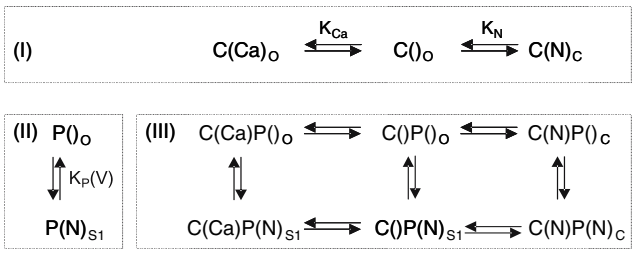

Fig. 4 Kinetic schemes for two neomycin inhibition mechanisms. *I*, Neomycin and Ca^{2+} bind to a cytoplasmic site on RyR1. The channel is open (subscript *O*) when the site is empty or occupied with Ca^{2+} (RyR1 can be activated by ATP even in the absence of Ca^{2+}). The binding of neomycin (*N*) to this site closes the channel (subscript *C*). *II*, Neomycin can lodge in the pore and partially block the ion conduction pathway, causing a conductance substate (subscript *S1*) as demonstrated by Mead & Williams (2002a). The blocking affinity depends on membrane voltage (*V*). *III*, The combination of the processes in schemes I and II represented as a six-state scheme

Table 1 Parameter values for model fits to single-channel data

Binding step	Affinity (μM)	K (10^6 M^{-1})
C site: Ca^{2+}, K_{Ca}	0.035[c]	27[c]
C site: neomycin, K_N	0.1[c]	10[c]
P site: neomycin, K_P	30,[a] 0.25[b]	0.033,[a] 4[b]

The relationship between RyR activity (p_o) and the model binding constants is given by the following equation: $P_o = P_{max}\left(\frac{1+K_{Ca}[Ca^{2+}]}{1+K_{Ca}[Ca^{2+}]+K_N[N]}\right) \times \left(\frac{1}{1+K_p[N]}\right)$

IC_{50} values were calculated numerically from this equation

[a] Obtained at 40 m*V*

[b] Obtained at –40 m*V*

[c] Values were voltage-independent

sites are 35 and 750 nM, respectively. This result indicates that neomycin competes either directly or allosterically with a new high-affinity Ca^{2+} binding site.

Effect of Neomycin on [^{3}H] Ryanodine Binding

We carried out [^{3}H]ryanodine binding assays to determine neomycin inhibition of RyR1 in the presence of the non-hydrolyzable ATP analogue AMP-PCP (Fig. 8). Neomycin decreased [^{3}H]ryanodine binding consistent with channel inhibition. This was measured under incubation conditions (*see* Experimental Procedures) that were intended to match as closely as practicable the conditions in the bilayer experiments (Fig. 8a). In contrast to the single-channel data (Fig. 2), the concentration dependence of neomycin inhibition of [^{3}H]ryanodine binding was biphasic. Phase 1 corresponded roughly to [neomycin] of 0.01-1 μM, whereas phase 2 was seen at [neomycin] of 10-1,000 μM. The data were analyzed with double Hill fits using the equation given in the caption to Figure 8. The Ca^{2+} dependence of the fit parameters is shown in Figure 8b and c. The magnitude of phases 1 and 2 (B_1 and B_2, respectively) plotted against cytoplasmic $[Ca^{2+}]$ (Fig. 8b) revealed that B_1 and B_2 were increased by cytoplasmic $[Ca^{2+}]$ with a half-maximal activation of $\sim$1 μM, which corresponds with that of RyRs in bilayer experiments (Laver, 2007). The half-inhibitory [neomycin] for phase 1 (K_1) is plotted against cytoplasmic $[Ca^{2+}]$ in Figure 8c. K_1 increased with increasing cytoplasmic $[Ca^{2+}]$, reminiscent of the IC_{50} for neomycin in single-channel experiments shown in Figure 3.

Discussion

Single-channel measurements (Figs. 1-3) indicate that *trans*-membrane voltage and *cis* $[Ca^{2+}]$ both affect the IC_{50} for *cis* neomycin inhibition. At $[Ca^{2+}]$ exceeding 0.1 μM, the IC_{50} for neomycin inhibition of RyR1 is similar to that reported for cardiac RyRs (RyR2) in the presence of $\sim$10 μM $[Ca^{2+}]$ (Mead & Williams, 2002a, 2002b, 2004). Their finding that neomycin preferentially blocks single-channel conductance at positive (40 m*V*) voltage steps suggests that neomycin binds to RyR2 within the *trans*-membrane electric field (Mead & Williams, 2002a). The fact that membrane potentials larger than 40 m*V* relieve neomycin block suggests neomycin permeation through the RyR pore when the driving force is sufficiently large (Mead & Williams, 2002a). Previous single-channel recordings have revealed that neomycin causes a conductance substate ($\sim$10% of maximum RyR2 conductance), indicating that plugging of the pore is incomplete (Mead & Williams,

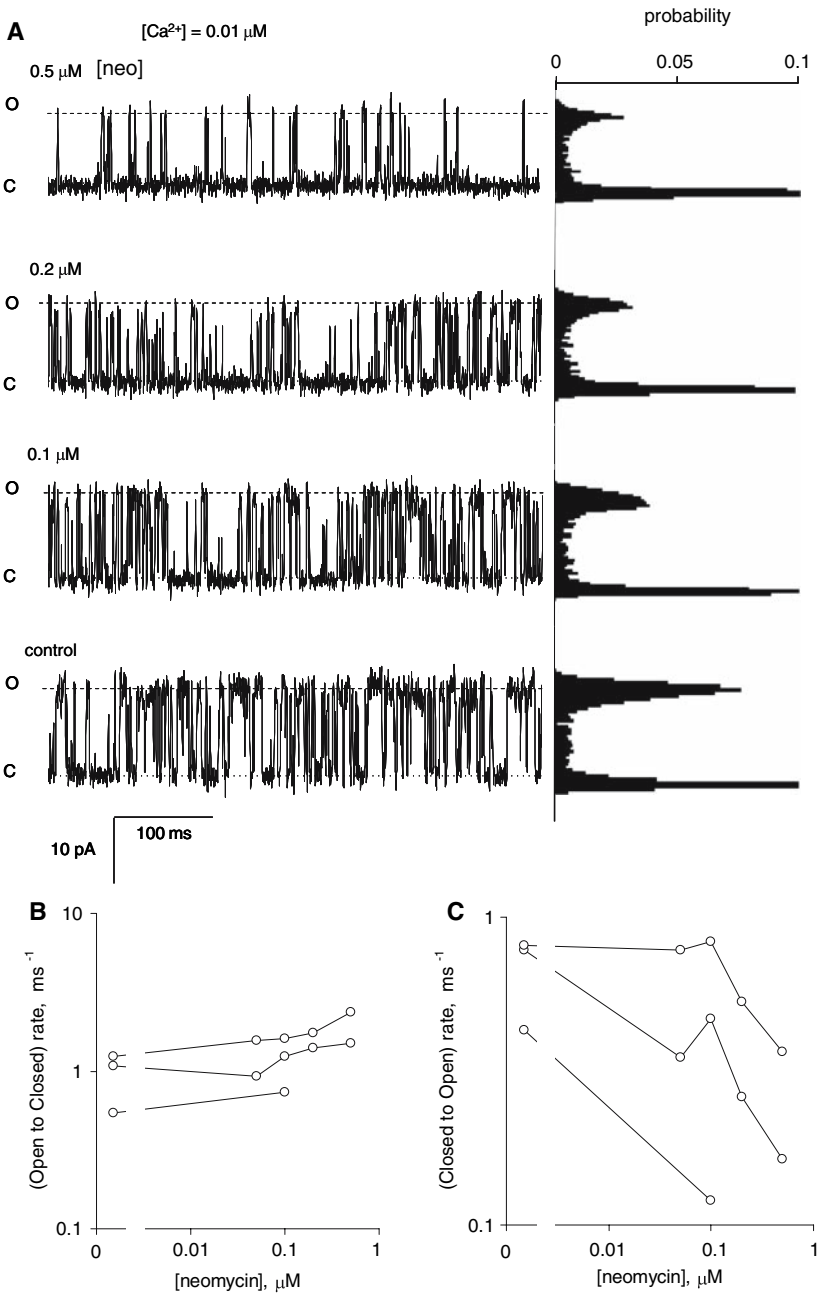

Fig. 5 RyR1 gating in response to neomycin inhibition in the presence (cytoplasmic) of 2 mM ATP and 0.01 μM Ca^{2+} at +40 m*V*. (**a**) Single-channel recordings of RyR1 in the presence of various concentrations of neomycin. The concentrations are given at the left of each trace. The recordings are shown on a time scale that shows the current transitions between the fully open level (*O*) and the closed (*C*) state. Amplitude histograms from longer episodes ($\sim$10 s) are alligned with recordings at the right of each trace. The size of each peak indicates the probabilities of the corresponding conductance states of the channel. Channel closing (**b**) and opening (**c**) rates were determined from HMM analysis of single-channel recordings. Data points from three individual experiments ($[Ca^{2+}]$ = 10 nM) are connected by lines

2002a). We show that in native RyR1, when *cis* $[Ca^{2+}]$ exceeds 0.1 μM, neomycin inhibits RyRs primarily by inducing a 30% conductance substate. Overall, neomycin inhibition at cytoplasmic $[Ca^{2+}]$ >0.1 μM is very similar to that observed in RyR2 and supports the conclusion that neomycin acts as a plug in the pore of RyR1.

In contrast, the neomycin IC_{50} seen at submicromolar $[Ca^{2+}]$ appears to be strongly influenced by the competition between neomycin and Ca^{2+} binding to a common cytoplasmic site. While high $[Ca^{2+}]$ (>0.1 μM) most likely competes out neomycin binding to this site (which is why we only observe pore plugging by neomycin at these Ca^{2+} levels), at low Ca^{2+} neomycin most likely binds to a regulatory site that lies outside the *trans*-membrane electric field, given the weak voltage dependence of this form of inhibition. This inhibition mechanism produces channel closures with zero conductance, which is quite different from the substates caused by the pore plugging mechanism. The *cis* Ca^{2+} dependence of neomycin IC_{50} indicates that the neomycin/Ca^{2+} site has a Ca^{2+} affinity that is 30-fold higher than has been attributed to the Ca^{2+} activation sites of RyR1. This indicates that neomycin binds to a previously uncharacterized Ca^{2+} binding site. The lack of involvement of the Ca^{2+} activation site in neomycin

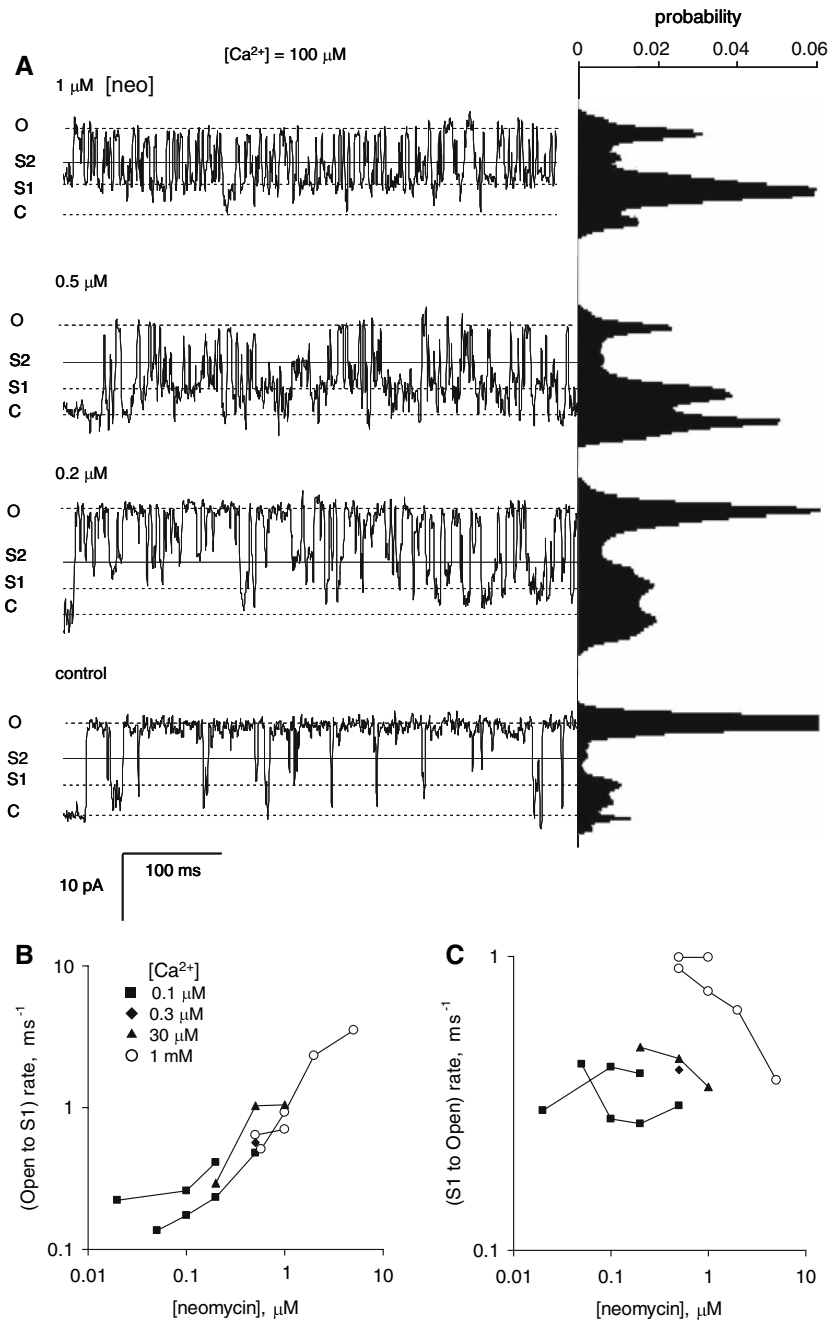

Fig. 6 RyR1 gating in response to neomycin inhibition in the presence (cytoplasmic) of 2 mM ATP and 100 μM Ca^{2+} at +40 m*V*. The data are displayed as described in the legend to Figure 5. (**a**) Single-channel recordings of RyR1 in the presence of increasing concentrations of neomycin. The recordings are shown on a time scale that shows the current transitions between the fully open level (*O*) and closed (*C*) and subconductance (*S1* and *S2*) states. The peaks in the amplitude histograms indicate the various conductance states of the channel. HMM analysis detected substates with conductances of 33% (S1) and 70% (S2) of the fully open conductance. Addition of neomycin primarily caused an increase in the S1 peak in the amplitude histograms, indicating that neomycin induces the S1 substate. Channel closing (**b**) and opening (**c**) rates between the S1 and open states. Data points from individual experiments are connected by lines. Experiments were carried out using cytoplasmic [Ca^{2+}] of 0.1 μM (■), 0.3 μM (◆), 30 μM (▲) and 1 mM (○)

inhibition was also concluded by Mack et al. (1992) on the basis that neomycin did not alter the half maximal effective concentration (EC_{50}) of Ca^{2+} activation of RyR1.

The dual mechanism for neomycin inhibition as described by scheme III (Fig. 4) quantitatively accounts for the [Ca^{2+}] dependence of neomycin IC_{50} determined from the neomycin dose-response of p_o. It also predicts that the [neomycin] dependence of p_o is monophasic, as seen in Figure 2. However, the mean current through the channel can have a biphasic [neomycin] dependence (we have not measured this directly due to the limited precision of mean current determined from single-channel recordings). For example, pore plugging will cause partial inhibition of mean current with an IC_{50} of $\sim$1 μM (the first phase of inhibition), whereas further inhibition via the allosteric mechanism will become apparent as [neomycin] is increased beyond 10 μM (–40 m*V* and high [Ca^{2+}], the second phase of inhibition). On the other hand, at low [Ca^{2+}] the IC_{50} for allosteric inhibition is $\sim$0.1 μM so that it masks the pore plugging mechanism that occurs at higher [neomycin]. Therefore, at low [Ca^{2+}] allosteric inhibition is the dominant mechanism and the neomycin dose-response is monophasic. This would qualitatively account for the complex nature of neomycin inhibition of Ca^{2+} release

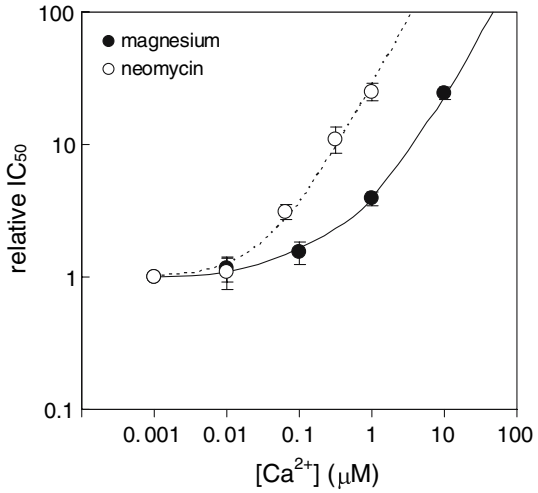

Fig. 7 The $[Ca^{2+}]$ dependence of IC_{50} for neomycin and Mg^{2+} inhibition of RyR1 in the presence of 2 mM ATP. Comparison of neomycin and Mg^{2+} inhibition at –40 m*V*. The Mg^{2+} data are taken from Laver, O'Neill & Lamb (2004). The plot shows the Ca^{2+}-dependent region of each data set normalized to the respective IC_{50} values at 1 nM Ca^{2+} (K_{Mg} = 40 ± 10 μM for Mg^{2+} and K_N = 100 ± 20 nM for neomycin). The data are fitted with the equation $IC_{50}/K_{N,Mg} = (1 + [Ca^{2+}]/K_{Ca})$ (*dashed* and *solid curves*) derived from scheme I in Figure 4. If neomycin and Mg^{2+} compete to the same Ca^{2+} site, then the Ca^{2+} dependence of the relative IC_{50} values for neomycin and Mg^{2+} should be identical. *Solid* and *dashed curves* are quite different, indicating competition at two distinct Ca^{2+} sites with affinities (K_{Ca}) = 35 nM and 750 μM, respectively

from SR vesicles (*see* Fig. 4 in Calviello & Chiesi, 1989) that exhibited a monophasic dose-response with an IC_{50} of 0.37 μM at 2 μM cytoplasmic Ca^{2+} and a biphasic dose response with an additional IC_{50} at 4.5 μM when cytoplasmic $[Ca^{2+}]$ was elevated to 30 μM.

Although the mechanisms of neomycin inhibition of ryanodine binding are not yet clear, the biphasic neomycin inhibition of ryanodine binding (Fig. 8 and previous data by Mack et al., 1992) might have a similar explanation as biphasic neomycin inhibition of Ca^{2+} release and mean current (*see above*). For example, if plugging of the pore by neomycin only causes partial inhibition of ryanodine binding (analogous to the S1 substate in single channels) and allosteric inhibition completely prevents it (analogous to complete closure of single channels), then the ryanodine binding should exhibit a biphasic neomycin dose response.

Alternatively, different mechanisms could underlie the neomycin effects on ryanodine binding and channel open probability. However, phase 1 of the neomycin inhibition of ryanodine binding had similar $[Ca^{2+}]$-dependent IC_{50} values (K_1) to those obtained from single-channel experiments (cf. Figs. 3 and 8c), suggesting that at least phase 1 in the [^{3}H]ryanodine binding assay is due to the effects of neomycin on p_o. Phase 2 of the dose response is most

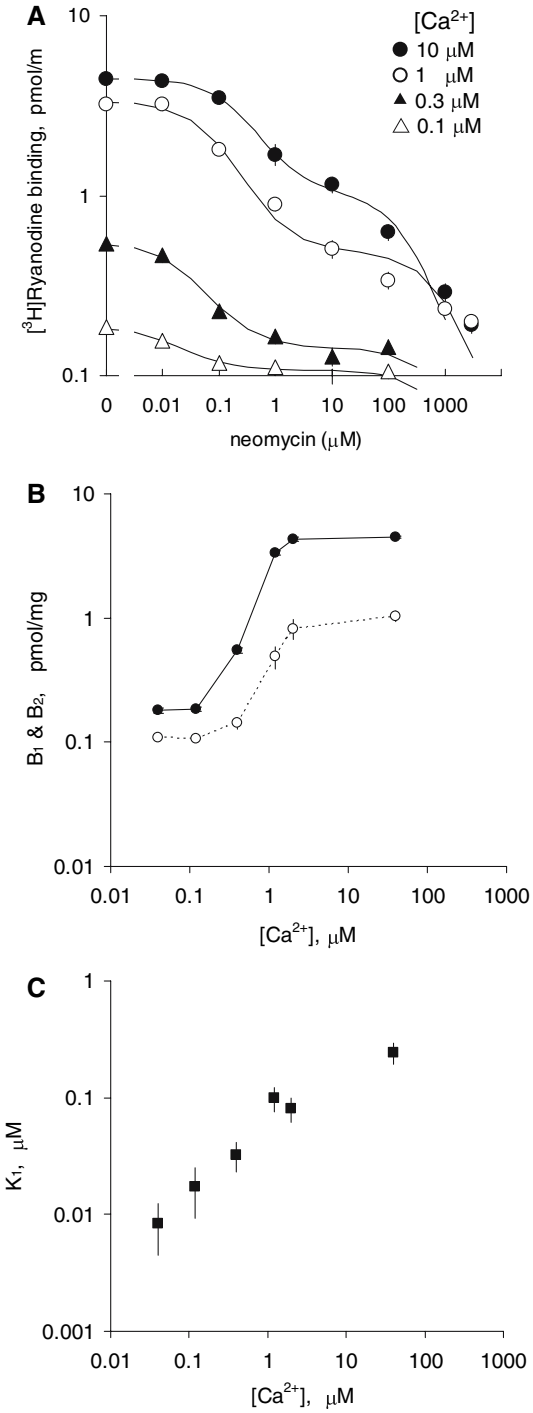

Fig. 8 The neomycin concentration dependence of [^{3}H]ryanodine binding to RyRs shows biphasic inhibition. (**a**) SR vesicles were incubated in 230mM $CsCH_3O_3S$, 20mM CsCl, 1 mM AMP-PCP, 10 mM TES (pH 7.4) and the indicated $[Ca^{2+}]$ at 22°C for 12 h. Data points show the means and standard errors of three experiments . The dose responses were fitted to double Hill fits using the equation $Binding = (B_1 - B_2)/(1 + [neomycin]/K_1) + B_2/(1 + [neomycin]/K_2)$ (**b**) The Hill equation parameters B_1 (●) and B_2 (○) from neomycin dose responses. (**c**) K_1 from neomycin dose responses

apparent at elevated [Ca^{2+}] (*see* Fig. 8a), where pore plugging is also most apparent in single channels. This suggests that phase 2 could be due to interactions between neomycin and ryanodine that occur when neomycin plugs the pore. Such interactions might also account for the slowing of the ryanodine unbinding at high [neomycin] (Mack et al., 1992).

In conclusion, there is a new mode of neomycin inhibition of the RyR that involves binding to a site that is competitive with Ca^{2+}. Therefore, neomycin inhibits RyRs by a dual mechanism in which neomycin can both plug the RyR pore and bind to a cytoplasmic Ca^{2+} site to cause allosteric closure of the channel. The latter mechanism has revealed a new high-affinity class of Ca^{2+} binding site(s) on the RyR that mediates neomycin inhibition.

Acknowledgement We thank Dr. Graham D. Lamb for his valuable comments on the paper. This work was supported by NH&MRC (grant 234420), an infrastructure grant from NSW Health through Hunter Medical Research Institute and National Institutes of Health grants AR 16922 from NIAMS and HL072841 from NHLBI. D. R. L. was supported by a Senior Brawn Fellowship from the University of Newcastle.

References

Calviello G, Chiesi M (1989) Rapid kinetic analysis of the calcium-release channels of skeletal muscle sarcoplasmic reticulum: the effect of inhibitors. Biochemistry 28:1301–1306

Chen SR, Li P, Zhao M, Li X, Zhang L (2002) Role of the proposed pore-forming segment of the Ca^{2+} release channel (ryanodine receptor) in ryanodine interaction. Biophys J 82:2436–2447

Chu A, Dixon MC, Saito A, Seiler S, Fleischer S (1988) Isolation of sarcoplasmic reticulum fractions referable to longitudinal tubules and junctional terminal cisternae from rabbit skeletal muscle. Methods Enzymol 157:36–50

Chung SH, Moore JB, Xia LG, Premkumar LS, Gage PW (1990) Characterization of single channel currents using digital signal processing techniques based on hidden Markov models. Philos Trans R Soc Lond Biol 329:265–285

Fleischer S, Ogunbunmi EM, Dixon MC, Fleer EA (1985) Localization of Ca^{2+} release channels with ryanodine in junctional terminal cisternae of sarcoplasmic reticulum of fast skeletal muscle. Proc Natl Acad Sci USA 82:7256–7259

Ikemoto N, Kim DH, Antoniu B (1988) Measurement of calcium release in isolated membrane systems: coupling between the transverse tubule and sarcoplasmic reticulum. Methods Enzymol 157:469–480

Inui M, Saito A, Fleischer S (1987) Purification of the ryanodine receptor and identity with feet structures of junctional terminal cisternae of sarcoplasmic reticulum from fast skeletal muscle. J Biol Chem 262:1740–1747

Jenden DJ, Fairhurst AS (1969) The pharmacology of ryanodine. Pharmacol Rev 21:1–25

Kourie JI, Laver DR, Ahern GP, Dulhunty AF (1996) A calcium-activated chloride channel in sarcoplasmic reticulum vesicles from rabbit skeletal muscle. Am J Physiol 270:C1675–C1686

Laver DR (2007) Ca^{2+} stores regulate ryanodine receptor Ca^{2+} release channels via luminal and cytosolic Ca^{2+} sites. Biophys J 92:3541–3555

Laver DR, Baynes TM, Dulhunty AF (1997) Magnesium inhibition of ryanodine-receptor calcium channels: evidence for two independent mechanisms. J Membr Biol 156:213–229

Laver DR, O'Neill ER, Lamb GD (2004) Luminal Ca^{2+}-regulated Mg^{2+} inhibition of skeletal RyRs reconstituted as isolated channels or coupled clusters. J Gen Physiol 124:741–758

Mack WM, Zimanyi I, Pessah IN (1992) Discrimination of multiple binding sites for antagonists of the calcium release channel complex of skeletal and cardiac sarcoplasmic reticulum. J Pharmacol Exp Ther 262:1028–1037

Mead F, Williams AJ (2002a) Block of the ryanodine receptor channel by neomycin is relieved at high holding potentials. Biophys J 82:1953–1963

Mead F, Williams AJ (2002b) Ryanodine-induced structural alterations in the RyR channel suggested by neomycin block. Biophys J 82:1964–1974

Mead FC, Williams AJ (2004) Electrostatic mechanisms underlie neomycin block of the cardiac ryanodine receptor channel (RyR2). Biophys J 87:3814–3825

O'Neill ER, Sakowska MM, Laver DR (2003) Regulation of the calcium release channel from skeletal muscle by suramin and the disulfonated stilbene derivatives DIDS, DBDS, and DNDS. Biophys J 84:1674–1689

Pessah IN, Francini AO, Scales DJ, Waterhouse AL, Casida JE (1986) Calcium-ryanodine receptor complex. Solubilization and partial characterization from skeletal muscle junctional sarcoplasmic reticulum vesicles. J Biol Chem 261:8643–8648

Rousseau E, Smith JS, Meissner G (1987) Ryanodine modifies conductance and gating behavior of single Ca^{2+} release channel. Am J Physiol 253:C364–C368

Wang JP, Needleman DH, Seryshev AB, Aghdasi B, Slavik KJ, Liu SQ, Pedersen SE, Hamilton SL (1996) Interaction between ryanodine and neomycin binding sites on Ca^{2+} release channel from skeletal muscle sarcoplasmic reticulum. J Biol Chem 271:8387–8393

Xu L, Wang Y, Gillespie D, Meissner G (2006) Two rings of negative charges in the cytosolic vestibule of type-1 ryanodine receptor modulate ion fluxes. Biophys J 90:443–453

Yano M, el-Hayek R, Antoniu B, Ikemoto N (1994) Neomycin: a novel potent blocker of communication between T-tubule and sarcoplasmic reticulum. FEBS Lett 351:349–352